Real time quantum correlation functions. II. Maximum entropy numerical analytic continuation of path integral Monte Carlo and centroid molecular dynamics data

Goran Krilov and B. J. Berne
Department of Chemistry, Columbia University, 3000 Broadway, New York, New York 10027

(Received 28 July 1999; accepted 1 September 1999)

We propose a method which uses centroid molecular dynamics (CMD) [J. Cao and G. A. Voth, J. Chem. Phys. **100**, 5106 (1994)] real-time data in conjunction with the imaginary-time data generated using path integral Monte Carlo simulations in a numerical analytic continuation scheme based on the maximum entropy approach. We show that significant improvement is achieved by including short-time CMD data with the imaginary-time data. In particular, for a particle bilinearly coupled to a harmonic bath, these methods lead to significant improvements over previous calculations and even allow accurate determination of transport coefficients such as the diffusion coefficient and mobility for this system. In addition we show how maximum entropy method can be used to extract accurate dynamic information from short-time CMD data, and that this approach is superior to the direct Fourier transform of long-time data for systems characterized by broad, featureless spectral distributions. © *1999 American Institute of Physics.* [S0021-9606(99)51744-3]

I. INTRODUCTION

Techniques based on the Feynman path integral formulation of statistical mechanics[1] made it possible to use simulation methods such as Monte Carlo (MC) and molecular dynamics (MD) to compute equilibrium properties of quantum systems. These methods are known as path integral Monte Carlo (PIMC)[2] and path integral molecular dynamics (PIMD).[3] Still, there are many important properties of quantum systems, such as transport coefficients, light and neutron scattering cross-sections, dipole relaxation times, and reaction rates which are time-dependent. Moreover, for these properties experimental results are readily available.

In principle, the dynamics of a canonical quantum system is determined by the time evolution of the density operator. Attempts to use the path integral techniques have encountered a formidable obstacle known as ''the sign problem,'' since in real time one has to evaluate the rapidly oscillating integrals over $\exp(-iS[q(t)]/\hbar)$, which leads to an exponential error growth with time. Therefore relatively few attempts have been made at the direct evaluation of real-time path integrals.[4–6]

An alternative approach to directly computing real-time quantum dynamics is based on numerical analytic continuation to real time of the quantum Euclidean-time correlation functions.[7] These do not suffer from the sign problem and can therefore be easily determined through either PIMC or PIMD methods. Recently, it has been shown that Bayesian ideas can be used to deal with the ill-posed nature of continuing noisy Euclidean-time Monte Carlo data to real time. This approach is called the maximum entropy (MaxEnt) method.[8] Several studies have appeared using these techniques.[9–13] For example, the spectra and transport of solvated electrons have been predicted in this way as well as the dynamic properties of systems coupled to harmonic baths using the Zwanzig Hamiltonian.[14] These studies show that the MaxEnt method is able to do a reasonable job for systems in which the dynamical variable does not display strong quantum coherences; that is for systems that decohere rapidly. Even then, there are many difficulties and one must determine imaginary time-correlation functions within very small error limits. This can only be achieved with very long and expensive PIMC simulations.

Kim *et al.* have recently suggested[15] that by combining real-time dynamics for short times with imaginary-time dynamics for the entire range (up to $\beta\hbar$) of imaginary time in the Bayesian approach, one can get more accurate predictions of the dynamics. Kim *et al.* demonstrate this by adding artificial noise to mathematical models of the spectral density and performing the MaxEnt inversion on the data synthesized in this fashion. In this way, they circumvent the problem of computing real-time data in a condensed matter system. Moreover, they assign uniform errors for the full time. It is possible to use PIMC to determine real-time correlation functions for short time,[16] however, in order for such data to be useful in a numerical analytic continuation scheme, one must still be able to generate data with very small statistical errors. Unfortunately, existing real-time path integral Monte Carlo schemes have errors which grow exponentially in time. Thus real-time data can be determined with sufficient accuracy only for short time and it behooves us to show that such data will significantly improve the inversion. In addition, the results of Kim *et al.* suggest that in order to achieve improvement over using imaginary-time data alone, accurate real-time data must be available up to some short cutoff time. Since this cutoff time may vary with the quality of the imaginary-time data and the particular system studied, it is unclear whether quantum Monte Carlo schemes can be used to generate accurate real-time data for sufficiently long times and hence be useful in the Bayesian approach.

Due to the above difficulties we choose an approach

which avoids the problem of the direct computation of real-time correlation functions. Instead, we suggest using the centroid molecular dynamics method (CMD)[17–19] to approximate the real-time dynamics for short times. For this purpose, it is useful to introduce the Kubo transformed time-correlation function,[20]

$$\psi(t)=\frac{1}{\beta}\int_0^\beta d\lambda\langle A(t+i\lambda\hbar)A(0)\rangle, \tag{1}$$

where A is a general operator. In cases in which A is a linear function of the position and momentum, such as the position and velocity autocorrelation functions, it is known that CMD generates the exact Kubo transformed time-correlation functions for harmonic systems.[17,21] Thus we suggest that the CMD method could be used to determine the short real-time evolution of the corresponding Kubo transformed quantum correlation functions, which could then be used as input data for the numerical analytic continuation method. It should be noted that in the CMD approximation to the Kubo function, the errors do not grow exponentially with time. Of course, the CMD result will deviate systematically from the exact Kubo function for intermediate and long times in anharmonic systems.

In this article we first show that the use of the short-time dynamics of the Kubo transformed time correlation function when used with the imaginary-time data does indeed improve the inversion from imaginary to real-time. In the accompanying preceding paper[22] we show that, in addition to being exact for harmonic systems, CMD gives accurate results for short-time quantum dynamics for a range of highly anharmonic systems as well. The main aim of this article is to determine if CMD combined with PIMC can be used to generate accurate quantum correlation functions for an assortment of systems for which we know the exact answers.

In Sec. II we present the maximum entropy method in the form that was implemented in this work. In Sec. III we discuss the numerical analytic continuation from the combination of real and imaginary time data. In Sec. IV we apply this method to several test systems for which exact solutions to quantum dynamics are available. We conclude in Sec. V.

II. THE MAXIMUM ENTROPY METHOD

The maximum entropy (MaxEnt)[8,23] inversion method has been established as a method of choice for many problems which involve the construction of the solution from an incomplete and noisy data. The method itself requires only the knowledge of the transformation which relates the data and the solution. Furthermore MaxEnt allows one to include any prior knowledge about the solution in a logically consistent fashion. As such, MaxEnt is ideally suited for solving ill-posed mathematical problems. A particularly important class of such problems involves inverting integral equations of the type

$$D(\tau)=\int d\omega\ K(\tau,\omega)A(\omega), \tag{2}$$

where the kernel $K(\tau,\omega)$ is singular. In this case, if the data set $D(\tau)$ is noisy and incomplete, the solution $A(\omega)$, also referred to as the map, cannot be determined uniquely. Maximum entropy principles provide a way to choose the most probable solution consistent with the data through the methods of Bayesian inference. Typically, the data is known only at a discrete set of points $\{\tau_i\}$, and we likewise seek a map at a discrete set of points $\{\omega_j\}$. The Bayes theorem states that

$$\mathcal{P}(\mathbf{A}|\mathbf{D})\propto\mathcal{P}(\mathbf{A})\mathcal{P}(\mathbf{D}|\mathbf{A}), \tag{3}$$

where $\mathcal{P}(\mathbf{A}|\mathbf{D})$ is the posterior probability, or the probability of $\mathbf{A}$ given $\mathbf{D}$, $\mathcal{P}(\mathbf{A})$ is the prior probability, or the probability of $\mathbf{A}$ without the data. $\mathcal{P}(\mathbf{D}|\mathbf{A})$ is known as the likelihood function, and is the probability of reconstructing the data from a given map. In MaxEnt, $\mathcal{P}(\mathbf{A})$ is chosen to be the entropic prior

$$\mathcal{P}(\mathbf{A})\propto e^{\alpha S}. \tag{4}$$

Thus, in lieu of the data, the best solution would be the one that maximizes the information entropy S, the form of which is axiomatically chosen to be

$$S=\sum_j \Delta\omega\left(A_j-m_j-A_j\ln\frac{A_j}{m_j}\right). \tag{5}$$

In this formulation the entropy is measured relative to a default model $m(\omega)$ which should in principle contain prior information about the solution, and α is a positive regularization parameter. The normal form of the likelihood function assumes that the noisy data are independent and Gaussian distributed, and is given as

$$\mathcal{P}(\mathbf{D}|\mathbf{A})\propto e^{-\chi^2/2}. \tag{6}$$

Here χ^2 is the standard mean-squared deviation from the data

$$\chi^2=\sum_{i,j}\left(D_i-\sum_k K_{ik}A_k\right)[C^{-1}]_{ij}\left(D_j-\sum_k K_{jk}A_k\right), \tag{7}$$

where C_{ij} is the covariance matrix

$$C_{ij}=\frac{1}{M(M-1)}\sum_{k=1}^{M}(\langle D_i\rangle-D_i^{(k)})(\langle D_j\rangle-D_j^{(k)}), \tag{8}$$

with M being the number of measurements. For independent, Gaussian distributed data the covariance matrix is diagonal and χ^2 reduces to the familiar form

$$\chi^2=\sum_i\frac{\left(D_i-\Sigma_k K_{ik}A_k\right)^2}{\sigma_i^2}, \tag{9}$$

where σ_i are the standard deviations of each data point. In practice, the measured data often exhibit significant correlations and C_{ij} is not diagonal. In such a case, proper MaxEnt treatment requires that one find an orthogonal transformation U which diagonalizes the covariance matrix, and transform the kernel $K'=U^\dagger K$ and the data $\mathbf{D}'=U^\dagger\mathbf{D}$. The χ^2 function then reduces to the above form. Using the above results the posterior probability takes the form

$$\mathcal{P}(\mathbf{A}|\mathbf{D})\propto\exp(\alpha S-\chi^2/2)=e^Q. \tag{10}$$

The problem of finding the MaxEnt solution then involves finding a map $\mathbf{A}$ which maximizes Q and is therefore a maximization problem in N variables, where N is the num-

ber of points $\{\omega_j\}$ at which we want to evaluate the solution. The solution obtained in this way is still conditional on the arbitrary parameter α, which can be interpreted as a regularization parameter controlling the smoothness of the map. Large values of α lead to the result primarily determined by the entropy function and hence the default model. Small α in turn lead to a map determined mostly by the χ^2 and thus lead to a closer fitting of the data. The principal drawback is that, along with the data, the errors would be fit as well.

There are several approaches to selecting the appropriate value of the regularization parameter α. The original maximum entropy prescription required α to be selected in such a way that

$$\chi^2 = N_d, \tag{11}$$

where N_{d} is the number of data. This gives a solution that barely fits the data, i.e., the deviation of the fit at each data point is of the order of the standard error in the data. It is therefore proposed that such a solution should be free of the artifacts due to fitting the noise.

The most widely used method is the classic MaxEnt.[24] In this approach Bayesian inference is used to derive the posterior probability of α given a data set

$$\mathcal{P}(\alpha|\mathbf{D}) \propto \frac{1}{\sqrt{\det[\alpha I + \Lambda]}}\, e^{Q} P(\alpha), \tag{12}$$

with Λ being the curvature matrix of χ^2 in the entropic metric,

$$\Lambda_{ij} = \frac{1}{2}\sqrt{A_i}\,\frac{\partial^2 \chi^2}{\partial A_i \partial A_j}\,\sqrt{A_j}. \tag{13}$$

$P(\alpha)$, the prior distribution of α, is usually taken to be a constant or $1/\alpha$. Classic MaxEnt selects the solution which simultaneously maximizes $\mathcal{P}(\mathbf{A}|\mathbf{D})$ with respect to A and $\mathcal{P}(\alpha|\mathbf{D})$ with respect to α. The condition for the classic MaxEnt solution is given by the Skilling equation

$$-2\alpha S(\mathbf{A}) = \sum_i \frac{\lambda_i}{\alpha + \lambda_i}, \tag{14}$$

where λ_i are the eigenvalues of Λ. The sum on the right hand side of Eq. (14) is often called the number of good data, N_g, and is the number of effective independent measurements.

Another way of choosing α is based on the L-curve method.[25,26] In this context we regard α as a regularization parameter controlling the degree of smoothness of the solution, and entropy as the regularization function. The value of α is selected by constructing a plot of $\log[-S(\mathbf{A})]$ vs $\log \chi^2$. This curve has a characteristic L-shape, and the corner of the L, or the point of maximum curvature, corresponds to the value of α which is the best compromise between fitting the data and obtaining a smooth solution.

A modification of classic MaxEnt is the average entropy approach suggested by Bryan.[27] This method calculates the solutions by averaging the maps for different values of α over the distribution $\mathcal{P}(\alpha|\mathbf{D})$ and should hence be superior to the classic result in cases in which this distribution is broad.

In this work we used all of the above criteria for selecting the regularization parameter. We find empirically that the classic MaxEnt and the L-curve methods give best results for the systems studied. In particular, for systems which are characterized by a broad, featureless spectral distribution, our studies show that the L-curve method gives most reliable results, while the classic MaxEnt sometimes leads to over fitting of the data and consequently introduces spurious features in the spectrum. On the other hand, for systems characterized by relatively sharp spectra, we find that classic MaxEnt gives good results. The reason for this behavior is that α selected by the L-curve method tend to be higher than those predicted by classic MaxEnt, therefore leading to smoother spectra. In addition, we observe that the regularization parameters obtained by the L-curve method lie in the range of α over which the resulting spectra are fairly insensitive to the particular value of α. As such, the L-curve method seems to be a viable alternative to classic MaxEnt for some systems.

We find that the use of Bryan's average entropy method gives results very similar to those of classic MaxEnt, without significant improvement of the latter for all problems considered in this work. We do, however, employ a useful maximization algorithm due to Bryan,[27] which reduces the space in which the search for the solution is performed. The kernel is first factored using singular value decomposition $K = V\Sigma U^T$. The singular nature of the kernel ensures only a small number of eigenvalues of Σ will be nonsingular. Since the space spanned by the rows of K is the same as that spanned by the columns of U associated with nonsingular eigenvalues, the search for the solution can be performed in this singular space of dimensionality N_s, where N_s is the number of nonsingular eigenvalues. The solution in singular space is expressed in terms of the vector $\mathbf{u}$, which is related to the N dimensional map space via

$$A_i = m_i \exp\left(\sum_{k=1}^{N_s} U_{ik} u_k\right). \tag{15}$$

This exponential transformation is useful since it ensures the positivity of the solution.

In this study we use a flat default map, which satisfies a known sum rule, such as the integral over the spectral density. Other choices of $m(\omega)$ and their effect on the quality of the results will be the subject of future investigation.

III. NUMERICAL ANALYTIC CONTINUATION

The particular case of an ill-posed problem in this work involves the numerical analytic continuation of imaginary-time data to real time. This is an important problem, since while imaginary-time equilibrium dynamics is usually readily available through quantum Monte Carlo methods, any attempt to obtain real-time information directly is plagued by the ''sign problem,'' which leads to phase cancellations and exponential growth of numerical errors with time.

Within the linear response regime, the spectral density function $I(\omega)$ is related to the real-time position autocorrelation function through a Fourier transform

$$C(t)=\int_{-\infty}^{\infty} d\omega\ e^{-i\omega t} I(\omega). \tag{16}$$

If one continues this relationship to imaginary-time, by letting $t\rightarrow -i\tau$ it becomes a two-sided Laplace transform

$$G(\tau)=\int_{-\infty}^{\infty} d\omega\ e^{-\omega\tau} I(\omega). \tag{17}$$

In order to compute $I(\omega)$ from $G(\tau)$ we need to perform an inverse Laplace transform which is an ill-posed problem. An equivalent formulation can be given in terms of the displacement correlation function

$$R^2(\tau)=\langle |q(-i\tau)-q(0)|^2\rangle, \tag{18}$$

which can also be expressed as

$$R^2(\tau)=\frac{\hbar c}{4\pi^2}\int_{-\infty}^{\infty} d\omega \times \frac{\cosh[\beta\hbar\omega/2]-\cosh\left[\beta\hbar\omega\left(\frac{1}{2}-\frac{\tau}{\beta\hbar}\right)\right]}{\omega\sinh[\beta\hbar\omega/2]}\,\sigma(\omega), \tag{19}$$

where $\sigma(\omega)$ is the photon absorption cross-section in the dipole approximation.

The methods of MaxEnt have been successfully employed in the treatment of this problem for a variety of quantum systems such as various quantum lattice models,[10] and an excess electron solvated in water,[12] helium, and xenon.[11] More recently, vibrational relaxation and infrared lineshapes have been studied as well.[13] All of these applications use quantum Monte Carlo simulations to compute the imaginary-time correlation functions to be used as an input in the MaxEnt inversion scheme. The spectral density or the absorption cross-section are then regarded as maps or solutions to be predicted by MaxEnt.

One of the drawbacks of this approach is that extremely accurate Monte Carlo data is required to reproduce the lineshapes with a sufficient accuracy. Moreover, proper treatment of errors is essential for successful reconstruction, which requires accurate evaluation of the covariance matrix, since most path integral Monte Carlo algorithms introduce correlations in the data. It should be noted that it is often more difficult to evaluate the covariance matrix accurately than it is to compute the imaginary-time correlation functions.

Recently, Kim *et al.*[15] suggested a way of incorporating real-time information in the MaxEnt scheme. Their reasoning is based on the idea that, since imaginary-time data contains mostly information about low frequencies (due to a kernel which decays exponentially as a function of $|\omega|$), the inclusion of the short-time, real-time data (containing information about high frequencies) should complement the imaginary-time data and thus improve the quality of the reconstructed spectrum. Therefore they reformulate the problem in terms of the complex time position correlation function $F(t,\tau)$

$$F(t,\tau)=\int_{-\infty}^{\infty} d\omega\ e^{-i\omega t} e^{-\omega\tau} I(\omega). \tag{20}$$

In this formulation the value of $F(t,\tau)$ along the positive real axis $F(t,0)$ corresponds to $C(t)$ and along the negative imaginary axis, $F(0,\tau)$ to $G(\tau)$. Hence one could use both correlation functions as input data. Furthermore, in principle one could perform a complex time PIMC simulation and compute $F(t,\tau)$ on a region of the complex time plane. However, such simulations are not easy to perform, due to high computational demand and the sign problem. Nonetheless, the tests Kim *et al.*[15] performed on synthesized data for spectra consisting of several sharp Gaussians seem to show that including short-time, real-time data offers considerable improvement over imaginary-time data, especially in the cases of noisy data.

One problem with this approach is that it is by no means easy to determine the short real-time decay of a quantum correlation function from simulation. Berne *et al.*[16] have devised a MC method for computing this short-time decay but the errors in this method grow exponentially with time. On the other hand, it was observed[15] that in order to achieve noticeable improvement in the inversion, one needs to include reasonably accurate real-time data up to a certain short cutoff time. Therefore, unless this cutoff time is short compared to the time at which the errors become unreasonably large, the advantage of including short real-time data is doubtful, since it would involve the use of very noisy data of uncertain quality. Moreover, the cutoff time depends on the quality of the imaginary-time data and has yet to be determined for each system. Thus, instead of following this path, we propose a modified approach of using approximate real-time data, obtained readily via CMD, in the MaxEnt inversion procedure. We will return to the MC method in a subsequent publication.

The Kubo transformed position correlation function, a particular case of Eq. (1) when $A=q$, is related to the spectral density through

$$\psi(t)=\frac{1}{\pi}\int_0^{\infty} d\omega\cos(\omega t)\frac{(1-e^{-\beta\hbar\omega})}{\beta\omega} I(\omega). \tag{21}$$

In particular, our results in the preceding paper[22] demonstrate that CMD shows excellent short-time agreement with the quantum results even for highly anharmonic systems as suggested by Voth and Cao. It should therefore be possible to use the short-time CMD data in place of the Kubo function (to which the centroid correlation function is an approximation) and use MaxEnt methods to find the best map $I(\omega)$ which simultaneously satisfies both Eqs. (16) and (21). In addition we show how MaxEnt can be used to extract the dynamic information using only the short-time centroid position correlation function data.

IV. RESULTS FOR SEVERAL TEST SYSTEMS

In order to test the ideas of the previous section we performed MaxEnt computations for several test systems, using both simulation data and mock data synthesized from the exact quantum spectrum and corrupted by random Gaussian noise.

The imaginary-time results were obtained using the staging PIMC method. The correlation function data was block-averaged to remove the correlations between successive Monte Carlo steps, and the length of blocks was adjusted to ensure the Gaussian distribution of the data. This was checked by computing the skewness and the kurtosis of the block averages for each imaginary-time data point $\{\tau_i\}$. In all cases it was found that the data are within the norm of a Gaussian distribution. The corresponding covariance matrix was computed from the block averages using the Bootstrap method,[28] which allows accurate evaluation of the off-diagonal covariance matrix elements. This is important as it was found that, due to strong correlations between data for different imaginary-times, the spectral analysis of the covariance matrix is often unstable with eigenvalues spanning several orders of magnitude.

The centroid position correlation functions were computed by CMD as described in the preceding paper.[22] We find that CMD introduces correlations between successive real-time data which cannot be removed. In other words, the covariance matrix for CMD data is nearly singular with many negative off-diagonal elements and cannot be used to remove the correlations. In particular we note that any simulation technique based on molecular dynamics would introduce correlation between points belonging to the same trajectory, unless they are separated by a time longer than the correlation time of the system. Tests involving classical mechanics showed similar behavior. The only way we found to remove those correlations is to compute each time point using a different set of trajectories. However, the computational expense of this approach is enormous, particularly in the case of CMD. Tests using classical mechanics show that millions of short trajectories are needed to obtained results converged to a sufficient accuracy to be useful in a maximum entropy inversion scheme. Currently, it is computationally impossible to perform such calculations with CMD. For that reason, we used only the diagonal elements of the CMD covariance matrix in MaxEnt calculations.

It should be noted that the effect of ignoring the off-diagonal matrix elements on the quality of the inversion is somewhat uncertain, since we were unable to include them in our method for reasons described above. In general, the importance of the off-diagonal covariance matrix elements in maximum entropy inversion methods is still a matter of debate.[23,10,15] We do find, however, that for good quality imaginary-time data, setting the off-diagonal matrix elements to zero does not affect the results significantly. We therefore believe that similar behavior extends to the data in the real-time domain. Certainly, this is a point which requires further consideration.

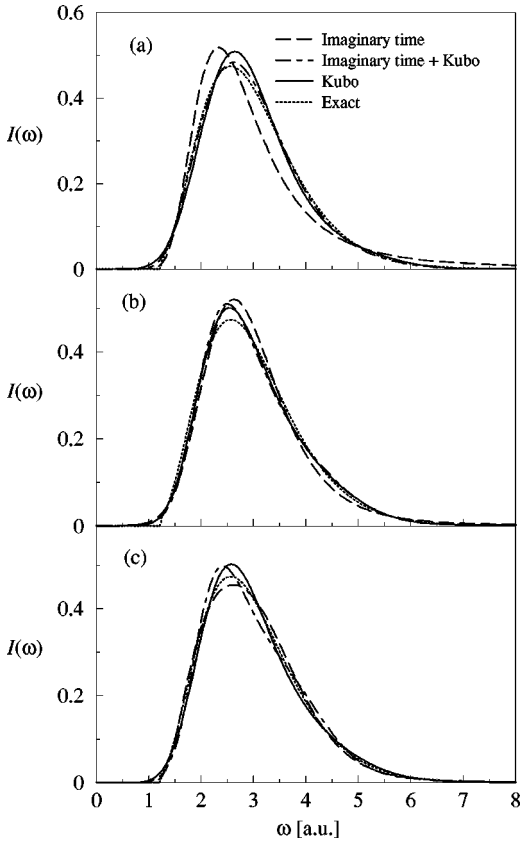

FIG. 1. The spectral density for a particle in a constant pressure 1D soft sphere potential with a weak harmonic component, with $P=1.0$ a.u. and $\beta=5.0$ a.u. The dotted line is the exact quantum result, the dashed line is the lineshape function computed by MaxEnt using imaginary-time data, the dot-dashed line is the spectral density computed by MaxEnt using the imaginary-time data and short-time Kubo transformed position correlation function as input, and the solid line is the result obtained by MaxEnt using only short-time Kubo function as input. All of the correlation functions were computed from the exact spectral density and corrupted by the addition of (a) 1%, (b) 0.1%, and (c) 0.01% Gaussian noise with respect to the maximum value of the functions.

A. Pressure-broadened line shapes

The first system we tested is the pressure-broadened line studied by CMD in the preceding work,[22] for the case of higher pressure $P=1.0$ a.u. We first constructed mock data from $I(\omega)$ computed numerically exactly, as described in the paper immediately preceding this one,[22] through the use of Eqs. (16) and (21). The Kubo function data included 30 points up to the real time of $0.3\,\beta\hbar$. The imaginary-time data was evaluated at 64 points up to $\tau=\beta\hbar/2$. We tested the MaxEnt inversion results for three different noise levels, 1%, 0.1%, and 0.01% with respect to the maximum values of the correlation functions. In each case we performed the MaxEnt inversion using the imaginary-time data only, the imaginary-time data in combination with short-time Kubo function data, and using only the short-time Kubo function data as input. For this particular system we find that the L-curve method gives most satisfactory results. Classic MaxEnt showed spurious features characteristic of over-fitting the data. The results are shown in Fig. 1.

Both the imaginary-time and the combination of imaginary-time and Kubo function data give very good re-

sults at all noise levels. Some improvement is noticeable for the combined data case, especially for the two large noise levels. At the smallest noise level, imaginary-time data itself gives very good results. What is unexpected is that the MaxEnt inversion of short-time Kubo function data by itself already gives an excellent reproduction of the dynamics, even at the largest noise levels, with the high frequency tail being particularly well reproduced. This result demonstrates that if the information about the essential features of the spectrum is contained within the short real-time data, the spectrum can be extracted efficiently through MaxEnt.

We next tested the same system using simulation data. In this case we used 128 imaginary-time data points for $G(\tau)$ calculated by PIMC with 2×10^6 passes. The correlations in imaginary time were removed by singular value decomposition of the covariance matrix. The Kubo function was approximated by CMD, from 10^4 trajectories. The real-time data was included up to 0.3 $\beta\hbar$. As in the case of the mock data we find that classic MaxEnt solutions exhibit spurious ringing features that tend to over-fit the data except for the case where CMD data is used as the sole input. These results are shown in Fig. 2(a). We instead used the L-curve method which gave results free from spurious features and these are given in Fig. 2(b).

Since the PIMC simulation data is quite accurate we see that the spectrum reconstructed from imaginary-time data alone already excellently reproduces the exact result. The combined data in this case shows a slightly less accurate performance with a spurious shoulder at the high frequency end. Once again, the short-time CMD data by itself gives an excellent reconstruction of the spectrum.

We next investigate how well we can reproduce the result using MaxEnt to extract information from short-time CMD data alone. Figure 3 shows the spectra reconstructed using MaxEnt for the cutoff in real time ranging from 0.1 to 0.5 in the units of $\beta\hbar$. We see that even for the shortest cutoff time of 0.1 $\beta\hbar$ we get a qualitatively correct result, whereas already for the cutoff time of 0.3 $\beta\hbar$, the spectrum is accurately reproduced. As we increase the cutoff time to 0.5 $\beta\hbar$ the exact result is recovered. One can compare these results with those shown in Fig. 5 of the preceding paper,[22] in which the lineshape function was computed by a direct Fourier transform of long-time CMD data. Such a result is much noisier and of poorer quality than the one obtained from short-time CMD through MaxEnt. We therefore propose this approach as a feasible alternative for extracting accurate dynamic information from CMD data. In particular, this approach would be well suited for systems such as those studied in the preceding paper,[22] for which the CMD results were shown to be reliable only for short-times.

B. Vibrational lineshapes

We next tested the method for the case of a homogeneously broadened line. In particular we look at the vibrational relaxation of a harmonic oscillator coupled to a harmonic bath. This system was already investigated in terms of the analytic continuation of imaginary-time data.[13] For this system it has been shown that the classical and quantum mechanical absorption cross-sections are identical.[29] The

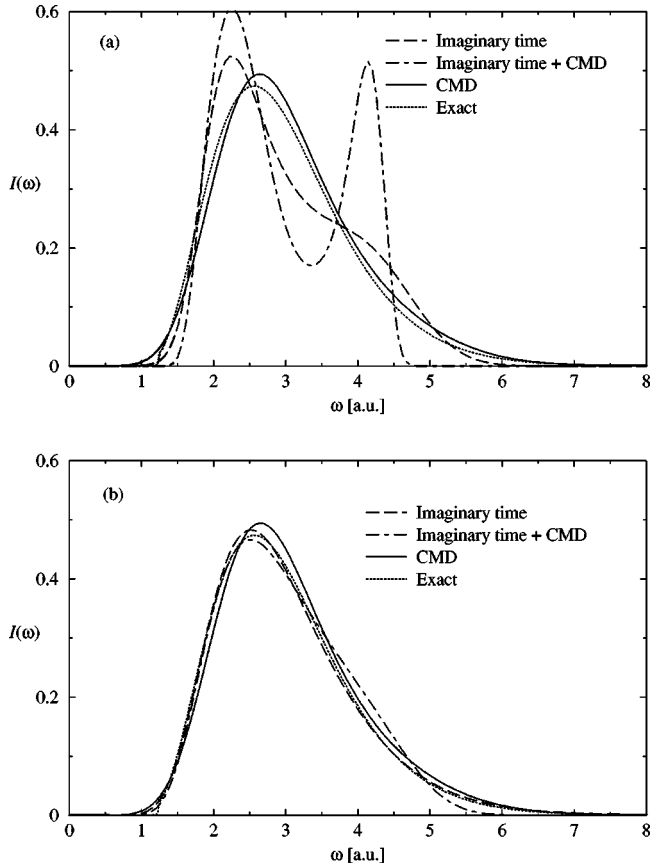

FIG. 2. The spectral density for a particle in a constant pressure 1D soft sphere potential with a weak harmonic component, with $P=1.0$ a.u. and $\beta=5.0$ a.u. The dotted line is the exact quantum result, the dashed line is the lineshape function computed by MaxEnt using imaginary-time data, the dot-dashed line is the spectral density computed by MaxEnt using the imaginary-time data and short-time centroid position correlation function as input, and the solid line is the result obtained by MaxEnt using only short-time centroid function. The imaginary-time correlation function was computed using PIMC and the centroid one using CMD. In (a) we show results obtained using classic MaxEnt and in (b) the corresponding results using the L-curve method.

classical cross-section can be calculated by solving the generalized Langevin equation[30] (GLE) and is given by

$$\sigma(\omega)=\left(\frac{8\pi}{mc}\right)\frac{\omega^2\gamma'(\omega)}{[\tilde{\omega}^2-\omega^2+\omega\gamma''(\omega)]^2+[\omega\gamma'(\omega)]^2}, \quad (22)$$

where $\tilde{\omega}^2=\omega_0^2-\zeta(0)/m$, γ' and γ'' are, respectively, the square of the renormalized frequency of the oscillator (from the potential of mean force), and the real and imaginary parts of the complex Laplace transform of the friction kernel $\zeta(t)$. The analytic form of the friction kernel chosen is that resembling an oscillator in a Lennard-Jones fluid,[13]

$$\zeta(t)=\zeta_0\{e^{-\alpha_1(ft)^2}[1+a_1(ft)^4]+a_2(ft)^4e^{-\alpha_2(ft)^2}\}. \quad (23)$$

It is worth remarking that the static friction ($\int_0^\infty dt\,\zeta(t)$) corresponding to this form of the dynamic friction scales as ζ_0/f. The particular parameters chosen are $\zeta_0=225$, $a_1=1.486\times10^5$, $a_2=285$, $\alpha_1=903$, and $\alpha_2=75.0$. In this

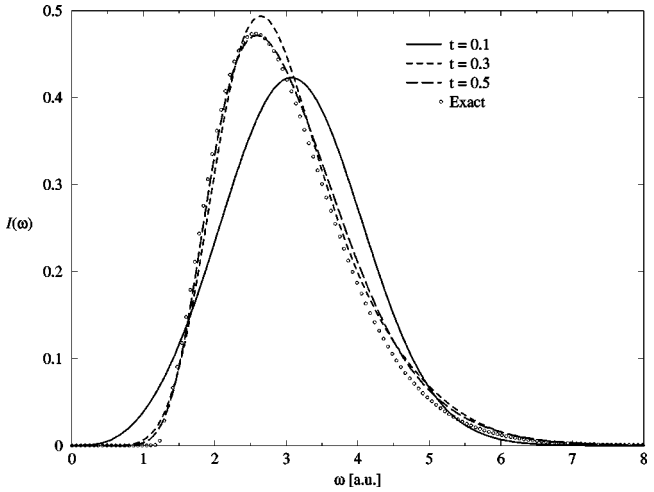

FIG. 3. The same system as in Fig. 2(b), except that input data only consists of short-time centroid position correlation data calculated by CMD. The real-time data was included up to $t=0.1$ (solid line), $t=0.3$ (dashed line), and $t=0.5$ (long-dashed line) in units of $\beta\hbar$. The empty circles are the exact quantum result for the spectral density.

study we consider two cases: high friction ($f=0.2$) and low friction ($f=1.0$) at the inverse temperature $\beta=1.0$ a.u. The bare oscillator frequency ω_0 was chosen to be 20 a.u. which was difficult to reconstruct by MaxEnt from imaginary-time data alone.[13] We constructed the mock imaginary-time data from $\sigma(\omega)$ using Eq. (19). Similarly, the Kubo function was constructed from

$$\psi(t)=\frac{c}{4\pi^2}\int_0^\infty d\omega\cos(\omega t)\frac{1}{\beta\omega^2}\sigma(\omega). \tag{24}$$

The data were corrupted by adding a specified amount of Gaussian noise (0.01%) relative to the maximum of the functions. Classic MaxEnt gave reliable results for this system and these are shown in Fig. 4. The imaginary-time data alone gives poorest agreement with the spectrum. On the other hand, we see that the inclusion of the Kubo function real-time data up to $t=0.3\,\beta\hbar$ improves the results considerably, particularly in the case of high friction. Once again we see that the short-time, real-time information contained in the Kubo function and extracted with the help of MaxEnt reproduces well the main features capturing both the oscillator peak as well as the low frequency phonon band present in the high friction case. The combined data gives the sharpest peak, as well as reproducing the tail regions well. In fact, we observe that the combined real- and imaginary-time data gives a better spectrum than the best imaginary-time case (10^{-5}% noise) reported.[13] One should note that for this system CMD would give the exact Kubo function since all the potentials are quadratic.

C. Transport coefficients

We next show how the aforementioned method of analytic continuation can be used to calculate transport coefficients, which are often difficult to obtain from real-time dynamics as they require reliable results for long times. In particular we look at the diffusion coefficient, which can be defined for a one-dimensional system as:

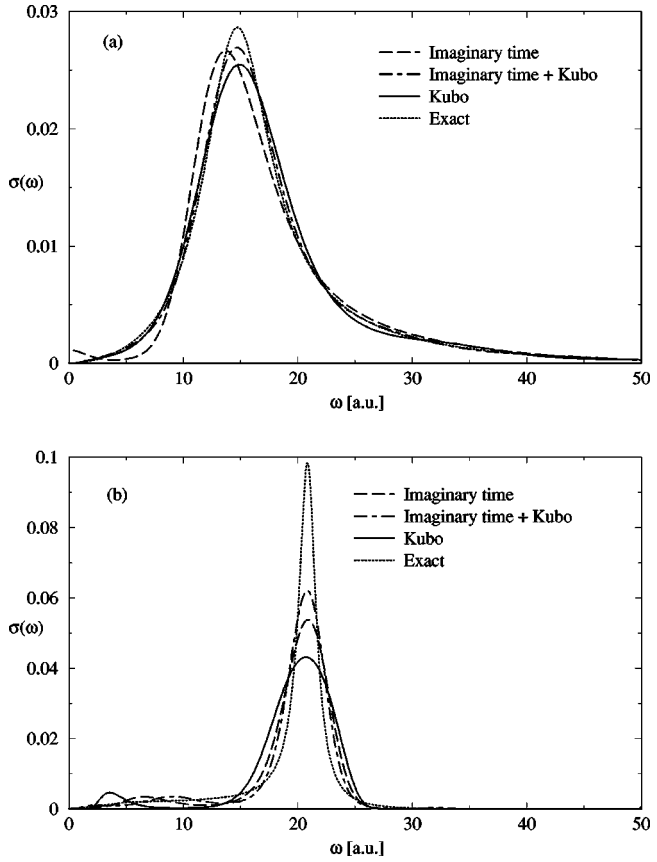

FIG. 4. Absorption cross-section for a linear harmonic oscillator bilinearly coupled to a harmonic bath. The dotted line is the exact quantum result, the dashed line is the cross-section computed by MaxEnt using imaginary-time data, the dot-dashed line is the spectrum computed by MaxEnt using the imaginary-time data and short-time Kubo transformed position correlation function as input, and the solid line is the result obtained by MaxEnt using only short-time Kubo function as input. The imaginary-time displacement correlation function and the real-time Kubo function were computed from the analytic result for $\sigma(\omega)$ for (a) $f=1.0$ (low friction) and (b) $f=0.2$ (high friction) case. The data were corrupted by addition of 0.01% Gaussian noise relative to the maximum value of the function. All the results were obtained using classic MaxEnt.

$$D=\lim_{s\to 0}\int_0^\infty dt\; e^{-st}\psi_v(t), \tag{25}$$

$\psi_v(t)$ being the Kubo transform of the velocity autocorrelation function. It has been shown[31] that the diffusion coefficient is proportional to the zero frequency absorption of the diffusing system,

$$D=\left(\frac{c}{8\pi\beta}\right)\sigma(0), \tag{26}$$

thereby D can be computed by evaluating $\sigma(0)$. The harmonic oscillator–harmonic bath system can be studied in the diffusive regime by letting the effective harmonic frequency of the system, $\tilde{\omega}$, go to zero. This can be achieved by choosing the bare frequency as

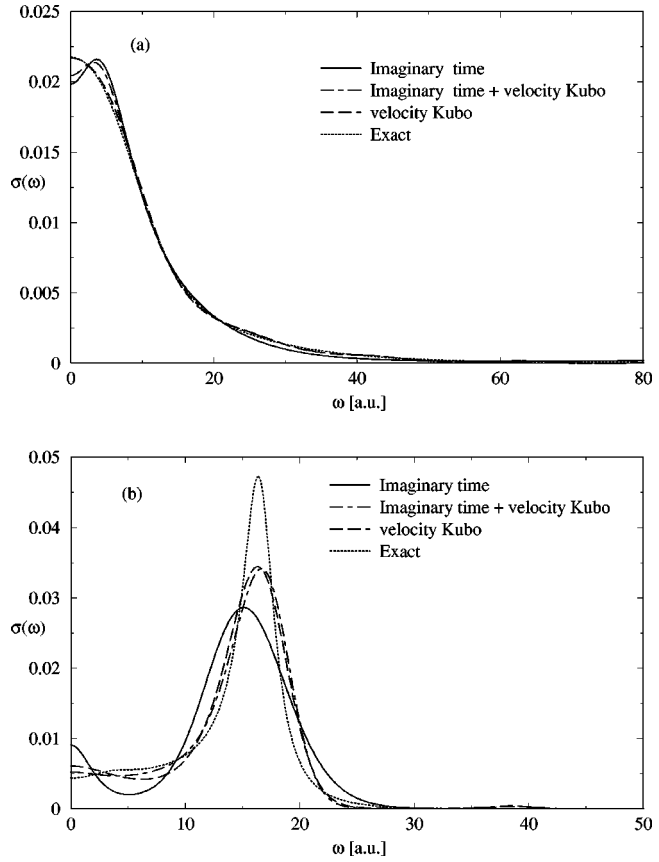

FIG. 5. The absorption cross-section of the system in Fig. 4, in the diffusive regime ($\tilde{\omega}=0$) which corresponds to oscillator frequency $\omega_0=15$ a.u. The input data were computed as in Fig. 4, except that real-time data was the short-time Kubo transformed velocity autocorrelation function. The data were corrupted by the addition of 1% Gaussian noise. Of particular interest is the zero frequency absorption $[\sigma(0)]$ which is related to the diffusion coefficient.

$$\omega_0^2=\zeta(t=0)/m=\zeta_0/m, \tag{27}$$

where the expression on the right hand side of this equation follows from Eq. (23). In this limit, the absorption cross-section takes the form

$$\lim_{\tilde{\omega}\to 0}\sigma(\omega)=\left(\frac{8\pi}{mc}\right)\frac{\gamma'(\omega)}{[\omega-\gamma''(\omega)]^2+[\gamma'(\omega)]^2}, \tag{28}$$

which is identical to the spectrum of a free particle coupled to a harmonic bath as given by the GLE. The absorption cross-section at zero frequency is finite and is given by

$$\sigma(0)=\left(\frac{8\pi}{mc}\right)\frac{1}{\gamma'(0)}. \tag{29}$$

In the particular case studied, $\tilde{\omega}=0$ limit was achieved by selecting the oscillator frequency $\omega_0=15$ a.u. We used the same method as in the case of $\omega_0=20$ a.u. discussed previously to compute $R^2(\tau)$ from the exact result for $\sigma(\omega)$. For real-time input, we used the short-time Kubo transformed velocity correlation function, computed from $\sigma(\omega)$, since the position correlation function is not defined for a diffusive system. In Fig. 5 we show the results for the high friction and low friction cases defined before. The exact correlation functions were corrupted by adding 1% Gaussian noise.

The results show that, even at such a large noise level MaxEnt predicts qualitatively correct spectra in all cases. For the low friction case, Fig. 5(a), the peak absorption is shifted to $\omega=0$ whereas for the high friction case, Fig. 5(b), the peak is shifted away from zero due to a large contribution from $\gamma''(\omega)$. In both cases imaginary-time data alone give qualitatively correct results, with accuracy being significantly better for the low friction case. The predicted values of the diffusion constant are $D=0.1082$ a.u. for the low friction case and $D=4.941\times10^{-2}$ a.u. for the high friction one. Combining the imaginary-time data with real-time velocity Kubo function information up to $t=0.3\,\beta\hbar$ shows improvement, particularly in the high friction case, predicting $D=0.1115$ a.u. (low friction) and $D=2.846\times10^{-2}$ a.u. (high friction). Using only short-time velocity Kubo information gives excellent results in both cases, particularly for the low friction case, in which it is the closest one to the exact spectrum. The diffusion coefficients computed in this fashion are $D=0.1182$ a.u. (low friction) and $D=3.693\times10^{-2}$ a.u. (high friction). These should be compared with the exact results of $D=0.1187$ a.u. and $D=2.378\times10^{-2}$ a.u. for the low friction and high friction case, respectively.

D. Overlapping Gaussian lineshapes

For the final test case, we considered a system whose absorption cross-section consists of two overlapping Gaussians, one centered at $\omega_1=20$ a.u. and the other at $\omega_2=30$ a.u. The half-width of the Guaussians was chosen to be 2.5 a.u. The imaginary-time and real-time Kubo functions are computed from the analytic form of this cross-section using Eqs. (19) and (24). The data were then corrupted by adding 0.1% Gaussian noise to the exact result.

Figure 6(a) shows the $\sigma(\omega)$ computed by classic MaxEnt using short-time Kubo function data, for real-time cutoffs ranging from 0.1 to 0.5 in units of $\beta\hbar$. The system was studied at the inverse temperature $\beta=1.0$ a.u. The shortest-time data is unable to resolve the peaks. However for the two longer times, the two frequencies are well resolved, and the correct lineshape is recovered. Note that the longest time shows excellent agreement with respect to the peak position. Also the higher frequency line shape is exactly reproduced, while the intensity of the lower frequency line is somewhat too high which is consistent with the notion that short-time, real-time data provides more information about higher frequencies.

In Fig. 6(b) we show the results for the case in which the combined imaginary-time and short, real-time Kubo function data were used as input, for two different values of the real-time cutoff. We observe that imaginary-time data alone cannot resolve the peaks, although the general positions of the peaks are captured. However, including even very short, real-time data (up to 0.1 $\beta\hbar$) already resolves the two frequencies. This best illustrates the advantage of using the Kubo function real-time data and the imaginary-time data in conjunction as neither of these two data sets by itself could resolve the frequencies. Including longer-time, real-time information once again leads to the recovery of the correct

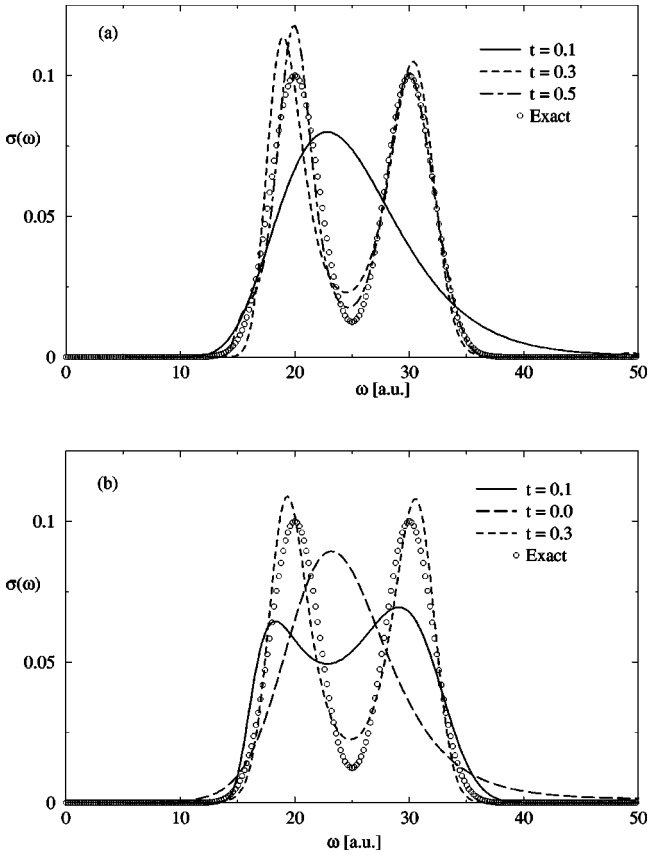

FIG. 6. Absorption cross-section consisting of two Gaussians, centered at $\omega=20$ a.u. and $\omega=30$ a.u., each of width 2.5 a.u. The empty circles show the exact result. In (a) we show the results obtained using MaxEnt with only the short-time Kubo function as input. The results in (b) were obtained using MaxEnt with imaginary-time data and short-time Kubo function data as input. The real-time data were included up to $t=0.1$ (solid line), $t=0.3$ (dashed line), and $t=0.5$ (dot-dashed line) in units of $\beta\hbar$. The long-dashed line in (b) corresponding to $t=0.0$ is the result for pure imaginary-time data. All data were computed from the exact $\sigma(\omega)$ and corrupted through the addition of 0.1% Gaussian noise.

lineshape, with an additional advantage that the recovered spectrum retains the symmetry of the exact result. The fact that both peaks are reproduced to the same accuracy also points to the complementarity of low and high frequency information in real- and imaginary-time data.

V. CONCLUSION

Based on the findings that CMD gives accurate results for short times[22] we propose, following the ideas of Kim *et al.*[15] on combining real- and imaginary-time data, to use both the short time CMD data and path integral Monte Carlo imaginary time dynamics data within the framework of numerical analytic continuation through maximum entropy inversion. We investigated a wide range of cases, using both simulation and synthesized data, which include inhomogeneously broadened soft sphere system, the vibrational relaxation of a harmonic oscillator coupled to a harmonic bath, the transport coefficients for the harmonic oscillator–harmonic bath system in the diffusive limit. We also tested the resolving powers of the method by analyzing a system whose absorption spectrum consists of two closely spaced broad Gaussians.

In contrast with the work of Kim and Doll, this study employed actual simulation data in addition to synthesized data. It should be noted that there are many difficulties associated with obtaining real-time data suitable for MaxEnt inversion from Monte Carlo simulations.[16] It is well-known that real-time PIMC simulations have errors which grow exponentially in time. Moreover, one must take care that these errors are independent and Gaussian distributed if the axioms of MaxEnt are to be applied correctly, both of which require large numbers of configurations to be generated. On the other hand, CMD provides a simpler and computationally less expensive way of obtaining approximate real-time data, which are not subject to the sign problem and therefore have little statistical noise, and which we find to be quite accurate for short times, even for highly anharmonic systems. This is especially true for large systems. On the other hand, CMD (in fact any MD based simulation) suffers from high correlations between different time data points, which cannot be removed through the usual covariance treatment. Nonetheless, we find that diagonal approximations to CMD covariance matrix gives reasonable results. Finding a way of better treating these correlations is a topic of future study.

We find that combining the imaginary-time data with short-time Kubo transformed real-time correlation functions leads to improvement in most cases. This improvement is most notable in cases where spectra exhibit sharp features such as the high friction case of the vibration–relaxation system [Fig. 4(b)], the corresponding diffusion case [Fig. 5(b)], and the case of closely spaced Gaussians (Fig. 6). We also find that in most cases, using short, real-time information alone, either generated from CMD or from the exact Kubo transformed correlation functions when these are available, we are able to, with the aid of MaxEnt, extract very accurate dynamic information about the system. This approach works particularly well in the case of broad featureless spectra, and may be a viable alternative to the direct Fourier transform in extracting information from the CMD data. In particular we show that with the MaxEnt approach, only short time (up to $0.3\,\beta\hbar$) is generally required to obtain reliable results.

In the context of CMD, such short-time information can be obtained from simulations with considerably less computational expense than long-time correlation data necessary for reliable Fourier transforms. This is particularly true if one is interested in transport properties such as diffusion coefficients and mobilities. In order to determine accurately the values of these from a dynamical simulation one usually needs to compute reliable long-time, real-time velocity or displacement correlation functions, which is, in the case of quantum systems, a formidable task. We find that, in cases of simple diffusion, it is possible with the aid of MaxEnt and CMD in conjunction with imaginary-time data, to obtain accurate (within 5% error) values for the diffusion coefficients using only very short (less than $0.5\,\beta\hbar$), real-time information. It should be noted that this approach would likely fail for more complicated transport processes such as barrier re-

crossing events or when long-time tails are present in the time correlation function. Nonetheless, it provides a significant advantage over long-time, real-time simulation approach for many systems of interest.

Finally, we point out a general trend in the quality of results in relation to different ways of including real-time data in the MaxEnt scheme. We note that combining imaginary-time data with short-time Kubo function data leads to most improvement when spectral features are sharp such as the case of harmonic oscillator–harmonic bath vibrational relaxation for the high friction case and in the corresponding diffusive limit as well as the system which has an absorption cross-section consisting of two closely-spaced Gaussians. These findings agree with the results of Kim and Doll for their spectra which consisted of sharp Gaussians. We find that in the case of broad spectral distributions, such as in the case of isobaric soft sphere system, the low friction harmonic oscillator–harmonic bath vibrational relaxation study and its corresponding diffusive limit, improvement seen by combining real- and imaginary-time data is marginal, except in the case of very noisy data, when the improvement is substantial [such as the case in Fig. 1(a)]. In these cases we believe it more prudent to apply MaxEnt methods directly to short-time Kubo function data on its own which gives excellent results in several cases, most notably for the diffusion coefficient in the low friction case of the oscillator-bath system [Fig. 5(a)]. Such an approach can be rationalized by recognizing that the MaxEnt method extracts all the available information from the short-time data. It then estimates the missing data by enforcing the smoothness of the spectrum. In the case of broad and smooth spectral distribution such estimates might be more accurate than fits to uncertain data available, for example, from imaginary-time simulations.

We also note that there is another way of combining short-, real-time data with Euclidean-time results in the MaxEnt scheme. One could compute the spectrum by performing MaxEnt inversion for short-, real-time data, and then use this spectrum as a default model $[m(\omega)]$ in MaxEnt inversion of the imaginary-time data. This approach will be an object of future study.

ACKNOWLEDGMENTS

This work was supported by a grant from the National Science Foundation. We would like to thank Dr. Eran Rabani for many useful discussions and Marc Pavese for helpful comments on the CMD method.

[1] R. P. Feynman and A. Hibbs, *Quantum Mechanics and Path Integrals* (McGraw-Hill, New York, 1965).
[2] H. F. Jordon, Phys. Rev. **171**, 128 (1968).
[3] M. Parinello and A. Rahman, J. Chem. Phys. **80**, 860 (1984).
[4] B. J. Berne and D. Thirumalai, Annu. Rev. Phys. Chem. **37**, 401 (1986).
[5] M. Topaler and N. Makri, J. Chem. Phys. **101**, 7500 (1994).
[6] C. H. Mak and R. Egger, J. Chem. Phys. **110**, 12 (1999).
[7] G. Baym and D. Mermin, J. Math. Phys. **2**, 232 (1961).
[8] *Maximum Entropy and Bayesian Methods*, edited by J. Skilling (Kluwer, Academic, Dordrecht, 1989).
[9] R. N. Silver, D. S. Sivia, and J. E. Gubernatis, Phys. Rev. B **41**, 2380 (1990).
[10] J. E. Gubernatis, M. Jarrell, R. N. Silver, and D. S. Sivia, Phys. Rev. B **44**, 6011 (1991).
[11] E. Gallicchio and B. J. Berne, J. Chem. Phys. **101**, 9909 (1994).
[12] E. Gallicchio and B. J. Berne, J. Chem. Phys. **105**, 7064 (1996).
[13] E. Gallicchio, S. A. Egorov, and B. J. Berne, J. Chem. Phys. **109**, 7745 (1998).
[14] R. Zwanzig, J. Stat. Phys. **9**, 215 (1973).
[15] D. Kim, J. D. Doll, and D. L. Freeman, J. Chem. Phys. **108**, 3871 (1998).
[16] D. Thirumalai and B. J. Berne, J. Chem. Phys. **81**, 2512 (1984).
[17] J. Cao and G. A. Voth, J. Chem. Phys. **100**, 5093 (1994).
[18] J. Cao and G. A. Voth, J. Chem. Phys. **100**, 5106 (1994).
[19] J. Cao and G. A. Voth, J. Chem. Phys. **101**, 6157 (1994).
[20] R. Kubo, N. Toda, and N. Hashitsume, *Statistical Physics II* (Springer, New York, 1985).
[21] S. Jang and G. A. Voth, J. Chem. Phys. **111**, 2357 (1999).
[22] G. Krilov and B. J. Berne, J. Chem. Phys. **111**, 9140 (1999), preceding paper.
[23] M. Jarrell and J. E. Gubernatis, Phys. Rep. **269**, 133 (1996).
[24] J. Skilling and S. F. Gull, Proc. Am. Math. Soc. **14**, 167 (1984).
[25] C. L. Lawson and R. J. Hanson, *Solving Least Squares Problems* (Prentice Hall, Englewood Cliffs, NJ, 1974).
[26] K. Miller, SIAM (Soc. Ind. Appl. Math.) J. Math. Anal. **1**, 52 (1970).
[27] R. K. Bryan, Eur. Biophys. J. **18**, 165 (1990).
[28] B. Efron and G. Gong, Am. Stat. **37**, 36 (1983).
[29] J. S. Bader and B. J. Berne, J. Chem. Phys. **100**, 8359 (1994).
[30] B. J. Berne, M. E. Tuckerman, J. E. Straub, and A. L. R. Bug, J. Chem. Phys. **93**, 5084 (1990).
[31] B. J. Berne, in *Physical Chemistry: An Advanced Treatise*, edited by H. Eyring (Academic, New York, 1971), Vol. VIIIB, Chap. 9, p. 539.